

# Screening and anti-screening effects in $J/\psi$ production on nuclei

K. G. Boreskov<sup>1)</sup>, A. B. Kaidalov<sup>1)</sup>

*Institute of Theoretical and Experimental Physics, 117218 Moscow, Russia*

Submitted 15 April 2003

Resubmitted 28 April 2003

Nuclear effects in  $J/\psi$  hadro- and electroproduction on nuclei are considered in framework of reggeon approach. It is shown that screening regime which holds for electroproduction at  $x_F \gtrsim 0.7$  and for hadroproduction at  $x_F \gtrsim -(0.2 \div 0.4)$  is changed with anti-screening regime for smaller  $x_F$  values.

PACS: 13.85.Ni, 24.85.+p

Heavy-quark production on nuclei provides an important information on strong-interaction mechanisms and is intensively discussed (see e.g. refs [1–3] for review of experimental data, discussion of some phenomenological models and more references). In this note we will discuss a phenomenon of changing screening regime to anti-screening one in  $J/\psi$  hadro- and electroproduction when  $x_\psi \equiv x_F$  decreases in the framework of the BCKT model [4, 5] based on the reggeon approach. For  $J/\psi$  hadroproduction it happens in the region of negative  $x_\psi$ . An investigation of this region can provide an important information on dynamics of charmonium production and may discriminate different dynamical models [2, 4, 6].

Nuclear effects are usually discussed in terms of conventional power-law parameterization  $F_A(x_\psi) \propto F_N(x_\psi) \cdot A^{\alpha(x_\psi)}$ , where  $F_N(x_\psi)$  ( $F_A(x_\psi)$ ) is inclusive  $J/\psi$  production cross section on a nucleon (on a nucleus). The function  $\alpha(x_\psi)$  characterizes nuclear effects at different longitudinal momentum fraction  $x_\psi$ .

Experimental data on  $J/\psi$  hadroproduction reveal a striking contradiction with simplest theoretical expectations. Experimentally [7–9] function  $\alpha(x_\psi)$  decreases from  $0.93 \div 0.95$  at  $x_\psi \simeq 0$  to values  $\sim 0.75$  at  $x_\psi \simeq 0.8$  thus indicating an increase of the absorption as  $x_\psi$  increases. Formation-time mechanism predicts an opposite behavior. Instead of expected scaling with  $p_{J/\psi}^{lab}$  experiment shows an approximate Feynman scaling with  $x_\psi$  [8]. Comparison of  $J/\psi$  production data at different energies exhibits an explicit breakdown of QCD factorization theorem for this process [10].

On the other hand when comparing  $x$  dependence of  $\alpha$  for  $J/\psi$  hadroproduction with one for light-quark particle hadroproduction (inclusive production of pions, nucleons, lambdas, etc.), one observes the same trend – a small absorption at  $x \simeq 0$ , large absorption at  $x \simeq 1$  and

approximate Feynman scaling. The difference is only quantitative one –  $\alpha$  is about  $0.4 \div 0.5$  at  $x \simeq 1$  for light quarks instead of  $\sim 0.7$  for heavy quarks. This behavior of  $\alpha(x)$  for light hadrons allows a natural explanation in Regge theory. Small absorption at  $x \sim 0$  is due to Abramovskii–Gribov–Kancheli (AGK) cancellation for inclusive spectra [11], and increasing absorption at high  $x$  is due to violation of AGK rules because of momentum conservation requirement [12].

In ref.[4] the model for heavy quark and lepton pair production was constructed taking into account the most essential aspects of reggeon approach. In the spirit of parton picture [13] it was suggested that a fast projectile looks due to quantum-mechanical fluctuations like a cloud of virtual particles consisting of light partons (quarks and gluons, or light-quark hadrons, mainly pions) and (with some small probability) of heavy partons (say  $c\bar{c}$  pair)<sup>2)</sup>. Different constituents of this fluctuation interact with nuclear matter and determine a dependence upon atomic number  $A$ . There are both elastic and inelastic interactions which from the viewpoint of reggeon diagrams are the different discontinuities of the same reggeon diagram. As a result there exist definite numerical relations between the discontinuities of different types (AGK rules [11]).

As it was stressed in ref.[4] one has to distinguish two types of reggeon diagram cuttings. For diagrams of the first class the registered particle is contained *inside* a pomeron and appears in intermediate state only due to cutting of this pomeron. In this case the AGK rules are always valid and all contributions of many-pomeron diagrams to inclusive spectra cancel. It happens because

<sup>2)</sup>In reggeon theory a mechanism of emitting these partons is supposed to be a multiperipheral one. Creation of heavy quarks in this model can be considered as an example of "intrinsic charm" mechanism which was discussed by Brodsky et al. [14, 10]. In reggeon approach one can consider on equal footing any heavy component (e.g. "an intrinsic lepton pair" and so on).

<sup>1)</sup>e-mail: boreskov@heron.itep.ru, kaidalov@heron.itep.ru

each additional pomeron can be both cut and uncut, and due to the opposite signs of inelastic and elastic rescatterings they cancel. As a result, only one-pomeron diagram contribution survives giving a linear  $A$  dependence of spectra. This situation is typical for low  $x$  particles.

Another situation occurs if a particle to be registered is contained inside “vertex” of reggeon diagram (we use a term “vertex” for part of diagram common for several pomerons attached to it). In this case AGK cancellation is not valid in general. The striking manifestation of this mechanism comes from  $A$  dependence of inclusive spectra at large  $x$  close to 1 (momentum conservation mechanism [12]). The fastest particles belong to the “vertex” but not to the pomeron, and corresponding discontinuities give  $\alpha \approx 1/3$  for large  $A$  compared to  $\alpha \approx 1$  for small  $x$ .

Similar effect exists if one observes the “vertex” particle of some particular type, e.g. the  $J/\psi$  meson. There are two sources of nuclear effects in this case [4]. The first one is connected with rescatterings of light partons in fluctuation on different target nucleons or, alternatively in the anti-laboratory frame, with fusion of fluctuations originated from different nucleons of fast nucleus. This mechanism plays a small role at present energies  $p_{lab} \lesssim 10^3$  GeV [4] and its contribution is inessential for anti-screening effects we are interested in.

Another contribution is connected to rescatterings of the charmed state itself. One of the important ingredient of the model of ref.[4] is an assumption that it is not the  $J/\psi$  meson that propagates along nucleus but some primary colorless system containing both  $c\bar{c}$  quarks (in color state) and light quarks (to screen this color charge). This state denoted as  $X$  can be  $D\bar{D}$  mesons, or  $D^*\bar{D}^*$  state or something else, but the crucial point is that this system is of large size and therefore strongly interacts with nucleons (with cross section of order of  $20 \div 30$  mb). Only at last stage this system  $X$  converts into  $J/\psi$  meson (or in  $\psi'$ ) which is registered experimentally. Note that large nuclear effects in observed  $J/\psi$  production at  $x \sim 1$  require large nuclear absorption cross section for any model. In our model these effects are due to large-distance non-perturbative dynamics.

After inelastic rescattering the state  $X$  can be lost for registration (e.g. due to conversion to a state with small projection into  $J/\psi$ ). One can describe this effect quantitatively introducing a probability  $\epsilon$  to find the state  $X$  after its inelastic rescattering. Then for  $\epsilon = 1$  one has exact AGK cancellation, for  $\epsilon = 0$  the situation is similar to momentum conservation mechanism for light mesons at  $x$  close to 1 (no AGK cancellation) with  $\alpha \simeq 1/3$ , and for  $0 < \epsilon < 1$  the situation is an intermediate one with incomplete AGK cancellation. Moreover, the momentum

of the state  $X$  decreases after each inelastic rescattering. This redistribution of the longitudinal momentum of the state  $X$  is essential for anti-screening effects discussed below.

Let us denote the momentum fraction distribution of system  $X$  immediately after its production as  $F_0(x)$ . The state  $X$  has some projection into state  $J/\psi$  (as well as into  $\psi'$ , etc.). The  $x_\psi$  distribution can be obtained from  $F_0(x)$  by convolution with some projection function  $G_\psi$ :

$$F_N^{(\psi)}(x_\psi) = F_1 \otimes G_\psi \quad (1)$$

where the notation was used

$$(f \otimes g)(x) = \int_x^1 \frac{dz}{z} f(z) g(x/z), \quad (2)$$

or, in the rapidity variables,

$$(f \otimes g)(\bar{y}) = \int_0^{\bar{y}} d\xi f(\xi) g(\bar{y} - \xi), \quad (3)$$

where  $\bar{y} = Y - y$  is a rapidity in the anti-lab frame.

The state  $X$  travelling through nuclear matter suffers both elastic and inelastic rescatterings. As in ref. [4] the change of  $x$  distribution due to inelastic rescattering will be described as a convolution with some function  $\epsilon G(z)$ , where  $G(z)$  is normalized ( $\int_0^1 G(z) dz/z = 1$ ), and the parameter  $\epsilon$  determines a probability to have again the state  $X$  after inelastic interaction (though with different momentum). After  $k$  inelastic rescatterings of the state  $X$  we have  $k$ -fold convolution:

$$F_k^{(\psi)} = F_1 \otimes \underbrace{\epsilon G \otimes \dots \otimes \epsilon G}_{k \text{ times}} \otimes G_\psi. \quad (4)$$

It is essential that the operation of convolution is commutative and associative, so we can first convolute  $F_1$  with  $G_\psi$  in the Eq.(4) and thus get the  $k$ -fold convolution of the  $J/\psi$  spectrum on the nucleon,  $F_N^\psi(x)$ , with rescattering functions  $G$ :

$$F_k^\psi = F_N^\psi \otimes \underbrace{\epsilon G \otimes \dots \otimes \epsilon G}_{k \text{ times}}. \quad (5)$$

In order to obtain the  $J/\psi$  inclusive spectrum on a nucleus, the functions  $F_k^{(\psi)}$  should be weighted with cross sections  $\sigma_A^{(k+1)}$  for  $k$  inelastic rescattering after  $X$  production:

$$F_A^\psi = \sum_{k=0}^{\infty} F_k(x_\psi) \sigma_A^{(k+1)}. \quad (6)$$

The explicit form of the weights  $\sigma_A^{(k+1)}$  depends upon energy region [4]. However the change  $\sigma_A^{(k+1)}$  is rather smooth and for simplicity we will use the same low-energy expressions as in ref.[4]:

$$\sigma_A^{(k+1)} = \sigma_{aN}^{(\psi)} \int d^2b \int_0^{T_A(b)} dv \exp(-v\sigma_X) (v\sigma_X)^k / k! , \quad (7)$$

where  $\sigma_{aN}^{(\psi)}$  is the cross section of  $J/\psi$  production on a nucleon,  $\sigma_X$  is the cross section of interaction of the state  $X$  with a nucleon, and  $T_A(b)$  is two-dimensional nuclear density as a function of impact parameter  $b$  (nuclear profile). These formulas correspond to rescatterings ordered in longitudinal direction (low-energy regime) and after summation over  $k$  give well known optical-type formula for the production cross section. Thus we come to Eq.(6) for  $J/\psi$  nuclear inclusive cross section where  $F_k(x)$  and  $\sigma_A^{(k+1)}$  are defined by Eqs.(5) and (7).

Let us discuss parameterizations of distribution functions entering the model. The function  $F_{aN}^\psi(x_\psi)$  can be determined from experimental data on  $J/\psi$  production on nucleon. Its form strongly depends on a type of a projectile  $a$ . For hadron beam it can be parameterized as

$$F_{aN}^\psi(x) = C_a(1-x)^{\beta_a} , \quad (8)$$

where  $\beta_\pi \simeq 2$  for pion and  $\beta_p \simeq 3$  for proton beam. For  $J/\psi$  production by photons (and electrons) the form of this function is strongly different: produced  $\psi$  particles are concentrated near  $x_\psi \simeq 1$ , and  $x_\psi$  distribution can be parameterized in a power-like way

$$F_{\gamma N}^{(\psi)}(x) = \beta_\gamma x^{\beta_\gamma} , \quad (9)$$

with  $\beta_\gamma \geq 6$ . We choose the value  $\beta_\gamma = 6$ .

As to the function  $G(x)$ , it is natural to suggest its similarity to the function  $F_{\gamma N}^{(\psi)}(x)$ . For simplicity we choose exactly the same form

$$G(x) = \beta x^\beta , \quad (10)$$

with  $\beta$  considered as a free parameter.

Terms of the series (6) in number of rescatterings  $k$  decrease fastly with  $k$ , and it is enough to take into account several first terms (4 ÷ 5). The corresponding convolutions at fixed impact parameter  $b$  are estimated analytically, and the  $b$  integration was performed numerically. We use for calculations the Woods-Saxon parameterization of nuclear density with standard values of parameters taken from ref.[15].

Before comparison of theoretical predictions with experimental data let us discuss firstly qualitative character of absorptive corrections. As we discussed above at small  $x \approx 0$  we have AGK cancellation, and the extent of its violation is proportional to  $1 - \epsilon$ , a probability to lose the state  $X$  after inelastic rescattering. The particle can be lost for registration not only if it disappears after interaction but also if it loses part of its momentum and is shifted into different region in  $x$ . As a result at large  $x$  values the AGK rules are violated and absorption effects can be observed (momentum conservation effect). However it is only redistribution (not a loss) of particles for the whole  $x$  region. For cross section integrated over  $x$  screening (absorption) effects are connected only with  $1 - \epsilon$  value but not with momentum conservation. For  $J/\psi$  photoproduction the absorption effects were usually analyzed only for integrated cross section and this is a reason for rather small values of effective cross sections extracted for  $J/\psi$  absorption (3 ÷ 5 mb). We want to demonstrate here<sup>3)</sup> that as a function of  $x$  nuclear effects can be rather big (with effective cross section of order of 20 ÷ 30 mb) but integrally they cancelled because of cancelling contributions from screening and anti-screening regions.

This is demonstrated at Fig.1 where we show description of the NMC data [16] on ratio  $R(\text{Sn}/\text{Be})$  of  $J/\psi$

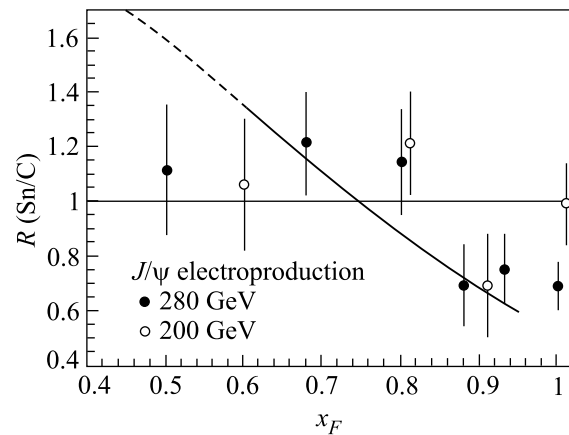


Fig.1. Description of data [16] on ratio  $R(\text{Sn}/\text{C})$  for  $J/\psi$  electroproduction. The curve corresponds to model calculations at parameter values  $\sigma = 30 \text{ mb}$ ,  $\epsilon = 0.85$ ,  $\beta = 12$

electroproduction cross sections as a function of  $x \equiv x_F$ . Since in this case the  $J/\psi$  spectrum is concentrated at  $x$  close to 1, the anti-screening regime takes place already at  $x \lesssim 0.8$ . Note that theoretical predictions at small  $x$  value ( $x < 0.6$ ) are less reliable due to their sensi-

<sup>3)</sup>First this phenomenon was discussed in the talk [5] based on our unpublished results.

tivity to small- $x$  parameterization of functions  $F_{\gamma N}^{(\psi)}$  and  $G(x)$ . Let us mention that our model is valid only for non-diffractive inclusive  $J/\psi$  production.

For  $J/\psi$  hadroproduction the anti-screening regime can be expected only for negative  $x$ . Fig.2a and Fig.2b show that for  $J/\psi$  and  $\psi'$  hadroproduction the change of regime happens at  $x \approx -(0.3 \div 0.5)$ . This value depends on parameters of the model – the less are momentum losses (the larger is  $\beta$ ) and the less is  $\epsilon$  the more negative  $x$ 's are necessary for the anti-screening onset (see Fig.2). For example, for the value of  $\beta = 4$  the crossover happens already at  $x \sim -0.2$ .

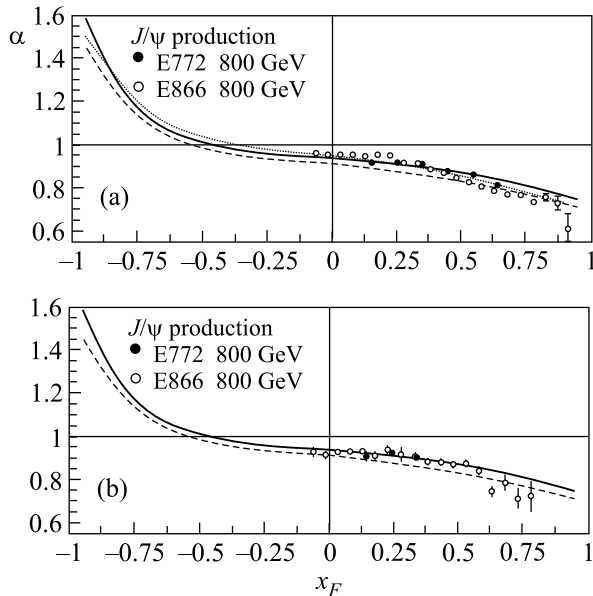


Fig.2. (a) Description of data [7, 8] on nuclear dependence of  $J/\psi$  hadroproduction. Curves correspond to model calculations for different ways of  $\alpha$  extraction: solid curve – from the ratio  $R(\text{Fe}/\text{C})$  and dashed curve – from  $R(\text{W}/\text{C})$ . The dotted line extracted from  $R(\text{W}/\text{C})$  corresponds to  $\epsilon = 0.95$ . (b) Description of data [7, 8] on nuclear dependence of  $\psi'$  hadroproduction. The curve corresponds to model calculations at parameter values  $\sigma = 30 \text{ mb}$ ,  $\epsilon = 0.85$ ,  $\beta = 12$

It is important to note that it is not entirely adequate to analyze such delicate effects as variation of dependence on atomic number with change of  $x$  or  $p_T$  in terms of the standard parameterizations  $A^\alpha$ . In general,  $\alpha$  is not only a function of  $x$  and  $p_T$  but depends also on atomic number  $A$ . This is demonstrated in Fig.2: there is a noticeable difference of solid and dashed theoretical curves which correspond to different choices of  $A$  ranges. Therefore the  $\alpha$  value extracted from experiments depends significantly on a chosen range of  $A$  and on a way of analysis. To exclude this uncertainty it is

preferable to compare with theory ratios of cross sections for different nuclei.

For simplicity we have considered only one primary state  $X$ . In approximation that all charmonia originate from this state nuclear effects should be universal for  $J/\psi$ ,  $\psi'$ , etc. In Fig.2b we give as an example a comparison of data on  $\psi'$  hadroproduction from refs [7, 8] with model calculation with a single  $X$  state at the same parameter values as in Fig.2a. Generalization to several primary states can lead to different  $A$  dependencies for different charmonia states.

Let us mention that in some theoretical models [2, 6] used for description of  $J/\psi$ ,  $\psi'$  hadroproduction in the negative  $x$  region the function  $\alpha(x)$  decreases (screening effects increase) as  $|x|$  increases in this region.

Thus, an experimental investigation of nuclear effects for charmonium production in the whole region of  $x$  can provide a valuable information for testing different dynamical models. In the reggeon approach one can distinguish three different regions in rapidity or in Feynman variable for  $J/\psi$  hadroproduction – in central region one has strong cancellation of screening diagrams and  $\alpha$  is close to one (small absorption cross section); at  $x > 0.2$  due to violation of cancellation rule the absorption effects increase and effective cross section is about  $20 \div 30 \text{ mb}$ ; at negative  $x$  less than  $-(0.3 \div 0.4)$  the anti-screening regime should be observed. Data on  $A$  dependence of charmonia production in the negative  $x$  region will be available soon from HERA-B experiment [17].

We are grateful to A. Capella and M. Danilov for stimulating discussions. This work has been partially supported by RFBR grants # 01-02-17383 and # 00-15-96786, INTAS grant # 00-00366 and DFG grant # 436 RUS 113/721/0-1.

1. R. Vogt, Phys. Rep. **310**, 197 (1999).
2. R. Vogt, Phys. Rev. **C61**, 035203 (2000); R. Vogt, Nucl. Phys. **A700**, 539 (2002).
3. B. Z. Kopeliovich and A. V. Tarasov, Nucl. Phys. **A710**, 180 (2002).
4. K. G. Boreskov, A. Capella, A.B. Kaidalov, and J. Tran Thanh Van, Phys. Rev. **D47**, 19-932 (1993).
5. K. G. Boreskov, in *Proc. of XXII Intern. Symposium on Multiparticle Dynamics*, Ed. C. Pajares, World Scientific, 1993.
6. D. Koudela and C. Volpe, hep-ph/0301186.
7. D.M. Alde, H.W. Baer, T. A. Carey et al., Phys. Rev. Lett. **66**, 133, 2285 (1991).
8. M. J. Leith, W. M. Lee, M. E. Beddo et al., Phys. Rev. Lett. **84**, 3256 (2000).
9. R. Shahoyan (NA50 Coll), hep-ex/0207014.

10. R. Vogt, S. J. Brodsky, and P. Hoyer, Nucl. Phys. **B360**, 67 (1991).
11. V. A. Abramovskii, V. N. Gribov, and O. V. Kancheli, Yad. Fiz. **18**, 595 (1973); [Sov. J. Nucl. Phys. **18**, 308 (1974)].
12. A. Capella and A. Kaidalov, Nucl. Phys. **B111**, 477 (1976).
13. V. N. Gribov, *Proc. of the VII LIYF Winter School of Physics* **11**, Leningrad, 1973, p. 5.
14. S. J. Brodsky and P. Hoyer, Phys. Lett. **B93**, 451 (1980).
15. A. Bohr and B. R. Mottelson, in *Nuclear Structure*, v.1, W. A. Benjamin, Inc., New York, Amsterdam, 1969.
16. P. Amaudruz, M. Arneodo, A. Arvidson et al., Nucl. Phys. **B371**, 553 (1991).
17. HERA-B: Report on Status and Prospects, DESY-PRC 00/04.